

Gas Analysis and Control Methods for Thermal Batteries

by Frank C. Krieger and Michael S. Ding

ARL-TR-6665

September 2013

NOTICES

Disclaimers

The findings in this report are not to be construed as an official Department of the Army position unless so designated by other authorized documents.

Citation of manufacturer's or trade names does not constitute an official endorsement or approval of the use thereof.

Destroy this report when it is no longer needed. Do not return it to the originator.

Army Research Laboratory

Adelphi, MD 20783-1197

ARL-TR-6665

September 2013

Gas Analysis and Control Methods for Thermal Batteries

Frank C. Krieger and Michael S. Ding
Sensors and Electron Devices Directorate, ARL

REPORT DOCUMENTATION PAGE				Form Approved OMB No. 0704-0188	
<p>Public reporting burden for this collection of information is estimated to average 1 hour per response, including the time for reviewing instructions, searching existing data sources, gathering and maintaining the data needed, and completing and reviewing the collection information. Send comments regarding this burden estimate or any other aspect of this collection of information, including suggestions for reducing the burden, to Department of Defense, Washington Headquarters Services, Directorate for Information Operations and Reports (0704-0188), 1215 Jefferson Davis Highway, Suite 1204, Arlington, VA 22202-4302. Respondents should be aware that notwithstanding any other provision of law, no person shall be subject to any penalty for failing to comply with a collection of information if it does not display a currently valid OMB control number.</p> <p>PLEASE DO NOT RETURN YOUR FORM TO THE ABOVE ADDRESS.</p>					
1. REPORT DATE (DD-MM-YYYY) September 2013		2. REPORT TYPE Final		3. DATES COVERED (From - To)	
4. TITLE AND SUBTITLE Gas Analysis and Control Methods for Thermal Batteries				5a. CONTRACT NUMBER	
				5b. GRANT NUMBER	
				5c. PROGRAM ELEMENT NUMBER	
6. AUTHOR(S) Frank C. Krieger and Michael S. Ding				5d. PROJECT NUMBER	
				5e. TASK NUMBER	
				5f. WORK UNIT NUMBER	
7. PERFORMING ORGANIZATION NAME(S) AND ADDRESS(ES) U.S. Army Research Laboratory ATTN: RDRL-SED-C 2800 Powder Mill Road Adelphi, MD 20783-1197				8. PERFORMING ORGANIZATION REPORT NUMBER ARL-TR-6665	
9. SPONSORING/MONITORING AGENCY NAME(S) AND ADDRESS(ES)				10. SPONSOR/MONITOR'S ACRONYM(S)	
				11. SPONSOR/MONITOR'S REPORT NUMBER(S)	
12. DISTRIBUTION/AVAILABILITY STATEMENT Approved for public release; distribution unlimited.					
13. SUPPLEMENTARY NOTES					
14. ABSTRACT <p>Gas analysis and control methods for the operating atmospheres of traditional pressed pellet and research thin-film thermal batteries are discussed. Thermal modeling combined with tests on the operating gas atmospheres of vendor pressed pellet munitions thermal batteries clearly shows that many vendor pressed pellet thermal battery lifetimes can be increased by factors ranging from 1.5 to 3 by hydrogen [H₂] gas removal even when using highly efficient microporous thermal insulation packages. An easily implemented method of H₂ gas removal from vendor thermal batteries is proposed.</p>					
15. SUBJECT TERMS Gas analysis, chromatography, thermal battery, heat transfer					
16. SECURITY CLASSIFICATION OF:			17. LIMITATION OF ABSTRACT UU	18. NUMBER OF PAGES 24	19a. NAME OF RESPONSIBLE PERSON Frank C. Krieger
a. REPORT Unclassified	b. ABSTRACT Unclassified	c. THIS PAGE Unclassified			19b. TELEPHONE NUMBER (Include area code) (301) 394-3115

Contents

List of Figures	iv
List of Tables	iv
Acknowledgments	v
1. Introduction	1
2. Experimental	2
3. GC/MS Calibration and Operation	3
4. Vendor Thermal Battery Gas Evolution	10
5. Summary and Conclusions	11
6. Future Work	12
7. References	13
List of Symbols, Abbreviations, and Acronyms	14
Distribution List	15

List of Figures

Figure 1. Calibration curve (2013) for pure O ₂ gas (forced origin method).	4
Figure 2. Calibration curve (2013) for pure O ₂ gas – slope/intercept method (FO = forced origin, SI = slope-intercept).	5
Figure 3. Schematic of enhanced gas handling system for use during 2014.....	12

List of Tables

Table 1. Slopes of dimensionless chromatographic peak areas (forced origin method) vs. measured gross gas sample pressures for pure gases and for gases from the certified calibration gas cylinder (including certified calibration cylinder volumetric gas percentages).	6
Table 2. Chromatographic curve areas (dimensionless) measured using the 50 µl sample loop for the certified gas cylinder calibration tests. These measured gas pressures all include the 0.5813 total volume fraction of argon gas in the certified gas cylinder.	7
Table 3. Individual gas pressures (torr) measured chromatographically for the gas samples shown in table 2 and taken from the certified calibration gas cylinder. Each individual gas pressure shown in table 3 includes a proportionate amount of the 0.5813 total volume fraction of argon gas in the certified gas cylinder.	8
Table 4. Moles of individual gases contained within the 50 µl sample loop for the gas samples shown in table 2 and taken from the certified calibration gas cylinder. The experimental temperature was taken at 298 °K for all of the molar calculations shown below. The molar volumes for all of the individual gases are 22.4140 std liter where $V = nRT/P = 1 \text{ mole} \times 62.3638 \text{ (l-Torr/mol-°K)} \times 273.15 \text{ °K}/760 \text{ Torr}$	8
Table 5. Percent errors of individual gases found under chromatographic curves when compared with the certified gas cylinder specifications for the gas samples shown in table 2 and comparisons of DCM total gross gas sample pressures with the sums of the pressures of the individual gases found under the chromatographic curves.	9

Acknowledgments

This work was funded in part by a Picatinny/Armament Research, Development, and Engineering Center (ARDEC) Technical Program Annex (TPA).

We would like to acknowledge the work of Rebecca Lennen for developing and calibrating the original gas chromatograph (GC) methods on the Hewlett Packard (HP) 5890 Series II GC as well as for her substantial assistance with instrumentation, thermal battery construction, and related technical assistance.

Bruce Poesse and Jennifer Mullins purchased the Agilent 7890A/5975C GC/mass spectrometer (MS), performed the original GC/MS setup and 7890A GC calibration, and provided GC/MS technical instruction and advice.

Ed Piekos and Anne Grillet of Sandia National Laboratories supplied advice and instruction on the Sierra Finite Element Thermal Battery Heat Transfer Mathematical Model.

INTENTIONALLY LEFT BLANK.

1. Introduction

Control of the operating gas atmospheres could achieve immediate and significant volume reduction and lifetime extension improvements for many vendor pressed pellet munitions thermal batteries. The importance of gas control in operating thermal batteries has been known and studied for many years (1–7), but gas control has not been actively pursued in pressed pellet munitions thermal batteries for the reasons explained below.

Present pressed pellet munitions thermal batteries using existing technologies can usually be engineered to meet present application volume requirements using traditional methods that are well known and highly effective. Control of the operating gas atmospheres is not inherently difficult, but it is a novel approach that requires experimental innovation in gas control, battery construction, chemical processing, and thermal modeling for optimal results.

The thermal battery industry is a relatively small, almost exclusively military, niche industry and innovative improvements in thermal batteries are not generally expected to produce large financial benefits. Decisions regarding thermal battery designs are usually made by production managers and engineers intent on meeting a near-term deadline for a specific application. Finally, the most obvious gas control methods require the difficult, but not impossible, guarantee that a low thermal conductivity gas atmosphere (or vacuum) be reliably maintained within a hermetically sealed thermal battery during the required 20-year shelf storage lifetime.

Although thermal battery technology is not inherently conducive to large financial gains, the batteries meet military munitions power, storage, and operational requirements for many missiles, artillery systems, and smart weapons. It is unlikely that thermal batteries will be replaced by other munitions power systems in the near future because of their high reliability, long shelf life, wide operating ambient temperature range, and relatively high energy and power densities. Measured energy and power density output values, based on the thermal cell stack only, for one high power U.S. Army Research Laboratory (ARL) thermal battery (MANLOS – required lifetime 120 s) were 79 Wh/kg, 248 Wh/l, 3.70 kw/kg, and 12.5 kW/l (6). Thermal cells can supply electrical loads of nominally 4 A/cm² of cell area at voltages of nominally 1.2 V/cell. Munitions thermal battery electrical outputs of nominally 30 V and 1 to 5 A are routinely drawn over operating times ranging from a few minutes to a few hours.

The relative ease of oxidizing H₂ gas to water during thermal battery initiation by using chemicals that can be easily incorporated into thermal battery construction (such as barium chromate [BaCrO₄]), and the fact that the resulting water vapor does not react with heated battery components to form significant amounts of additional H₂ gas in the operating Low Cost Competent Munition (LCCM) thermal battery was not conclusively demonstrated at ARL until recently (1, 2). The BaCrO₄ can be reduced to an ash that reacts readily with H₂ gas when the

battery is initiated by placing the BaCrO₄ into physical contact with heat paper that is ignited on battery activation. Removal of H₂ gas by oxidation with this BaCrO₄ ash would not require improvements in the presently used hermetic seals or any change in the shelf life gas composition during storage. The oxidizing BaCrO₄ ash would not exist until the thermal battery was initiated, so there would be no need to protect the oxidizing ash chemical surface during the required 20-year shelf life. This method of H₂ oxidation might immediately increase thermal lifetimes (or reduce required battery volumes) for many vendor pressed pellet thermal battery applications with only minor battery construction changes required.

The low operating temperature (−40 °C) under the most heat limited discharge conditions at low ambient temperature and the high mass of the LCCM thermal battery stainless steel (SS) reusable case fixture (low temperature rise during battery operation) tend to hold water vapor in the form of liquid or ice, and might have been contributing factors in the lack of production of additional H₂ gas from water vapor observed during the LCCM operating lifetime. Additional tests are needed to confirm the extent to which additional H₂ gas might be formed from water vapor in munitions thermal batteries with higher operating battery case temperatures.

If H₂ gas oxidation is to be effective in prolonging thermal battery operating lifetimes, the application must be heat limited and must have a small thermal insulation thermal mass (1, 4). Both of these conditions apply in many vendor pressed pellet munitions thermal batteries. In general, however, thermal battery operating lifetime (or miniaturization) improvements will be much more effective if additional gas control, thermal modeling, and traditional optimization methods are all used concurrently as has been previously reported (1–6).

This report primarily discusses ARL gas analysis methods as applied to pressed pellet thermal batteries. Thermal modeling clearly shows that simple removal of H₂ gas from the operating battery atmosphere could increase many vendor present pressed pellet thermal battery thermal and electrical lifetimes by factors ranging from 1.5 to 3 even when using the most efficient microporous thermal insulation packages (1, 4, 5) or reduce volume requirements significantly. More rigorous gas control methods combined with thermal modeling could either increase some present munitions thermal battery thermal lifetimes by a factor of about 10 or reduce the battery volume requirements much more significantly (6).

2. Experimental

Gas pressures in the gas handling system (GHS) used for gas sample collection were measured using an Agilent 34970A Data Acquisition/Switch Unit with Baratron dual capacitance manometer (DCM) pressure transducers (accuracy typically 1% or better) from MKS Instruments Incorporated. MKS DCMs were also used to measure the gas pressures directly at the GC. Gas evolution quantities were measured from the DCM pressures and known internal volumes of the

GHS that were measured using the ideal gas law with a 10-cc internal volume SS sample bottle (internal volume accurate to $\pm 10\%$) as a standard. Gas compositional analyses were done with an Agilent Technologies 7890A GC System using a thermal conductivity detector (typically 3 to 8 vol.% accuracy), and with an Agilent 5975C inert XL MSD (Triple-Axis Detector) Mass Spectrometer (MS). The GC and MS are contained within one Agilent instrument chassis, can be used individually or in combination, and the instrument is often referred to as a GC/MS analyzer. The sample gases used in the sample gas cylinder for the GC calibration were certified by the supplier as being accurate to 2.95% for each individual sample gas amount present. Ultra high purity (UHP) grade argon was the carrier gas used for the GC.

The GC used a Carboxen 1010 fused silica chromatographic porous layer open tubular (PLOT) capillary column (30 m long x 0.32 mm diameter x 15 μm average film thickness) from Supelco with a maximum isothermal operating temperature of 250 $^{\circ}\text{C}$ (catalog number 24246). A 10-cc SS sample bottle or a 25 cc gas syringe was used to supply gross gas samples to the GC. Gas sample pressures were measured using an MKS DCM directly connected to the GC system and gas was introduced onto the GC column using a 50- μl SS sample loop with a 6-port sample injection valve. Gas samples were introduced onto the MS column using a 50 μl Pressure-Lok gas syringe. The MS used an HP-5MS capillary column (crosslinked [5% phenyl] - methylpolysiloxane [30 m long x 0.32 mm diameter x 12 μm average film thickness with a maximum isothermal operating temperature of 325 $^{\circ}\text{C}$ – HP Part # 19091P – MS4]) from HP. Valco Instruments Company supplied the SS sample loop, the 6-port sample injection valve, and the gas syringes for the MS. UHP grade helium was the carrier gas used for the MS.

3. GC/MS Calibration and Operation

The GC/MS was purchased in December 2009, and the 7890A GC was installed, calibrated, and then used throughout 2010. The GC was calibrated for the six gases previously found in operating pressed pellet munitions thermal batteries (hydrogen [H_2], oxygen [O_2], nitrogen [N_2], carbon monoxide [CO], methane [CH_4], and carbon dioxide [CO_2]) at pressures ranging from about 20 to 850 Torr. If evolved sample gas pressures exceeded 850 Torr, the pressures were reduced to 850 Torr or less at the GC using a vacuum fore-pump before making a GC measurement.

The above six gases had previously been shown to constitute more than 94 % by volume of the evolved gases from the LCCM thermal battery using the older model HP 5890 GC (5). The 50- μl sample loop was used in both the 2010 and in the 2013 GC calibrations. For the 2010 calibrations, measured areas under the chromatographic curves of the above six pure gases were plotted against gas pressures measured by an MKS DCM attached to the operating GC. The slopes of the resulting curves showed linear regression R^2 values of 0.9983 or better. Those slopes were then used to confirm the known gas compositions of 50- μl gas samples from a

commercially purchased gas cylinder that contained known and certified quantities of all of the above six gases in argon. The original Agilent 7890 GC (2010) linear calibration curves were all forced through the origin, mostly for convenience of calculation, as is often done during GC calibrations (figure 1). A more accurate calibration method uses the slope-intercept method (figure 2). Figures 1 and 2 use exactly the same calibration data. Comparison of the peak areas from these two linear curves for O₂ shows that the peak area difference, as calculated from the two calibration curves, is less than the nominal 10% error of the total experiment for pressures greater than 25.7 Torr when the slope intercept linear curve is used as a basis with increased differences at pressures approaching 0 Torr. If the curve forced through the origin is used as a basis, the percentage differences near the origin are generally reduced slightly. The calibration numbers in this report are reported to more significant figures than justified to assist the reader in confirming the calibration details and results.

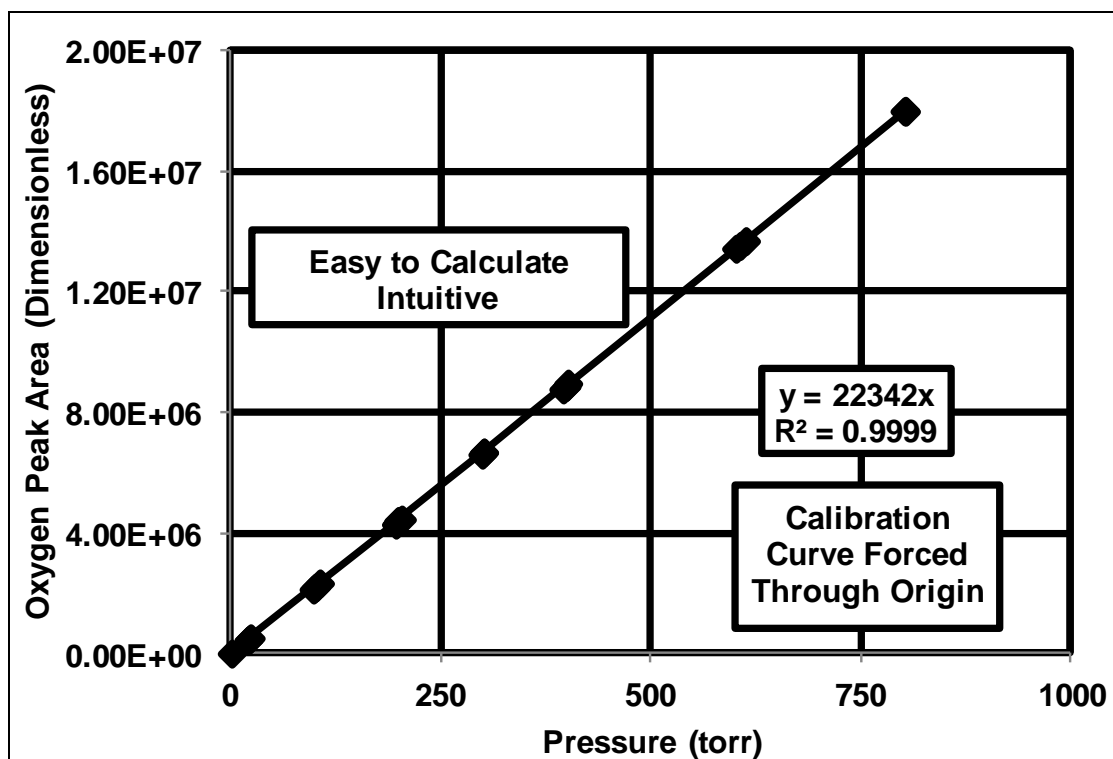


Figure 1. Calibration curve (2013) for pure O₂ gas (forced origin method).

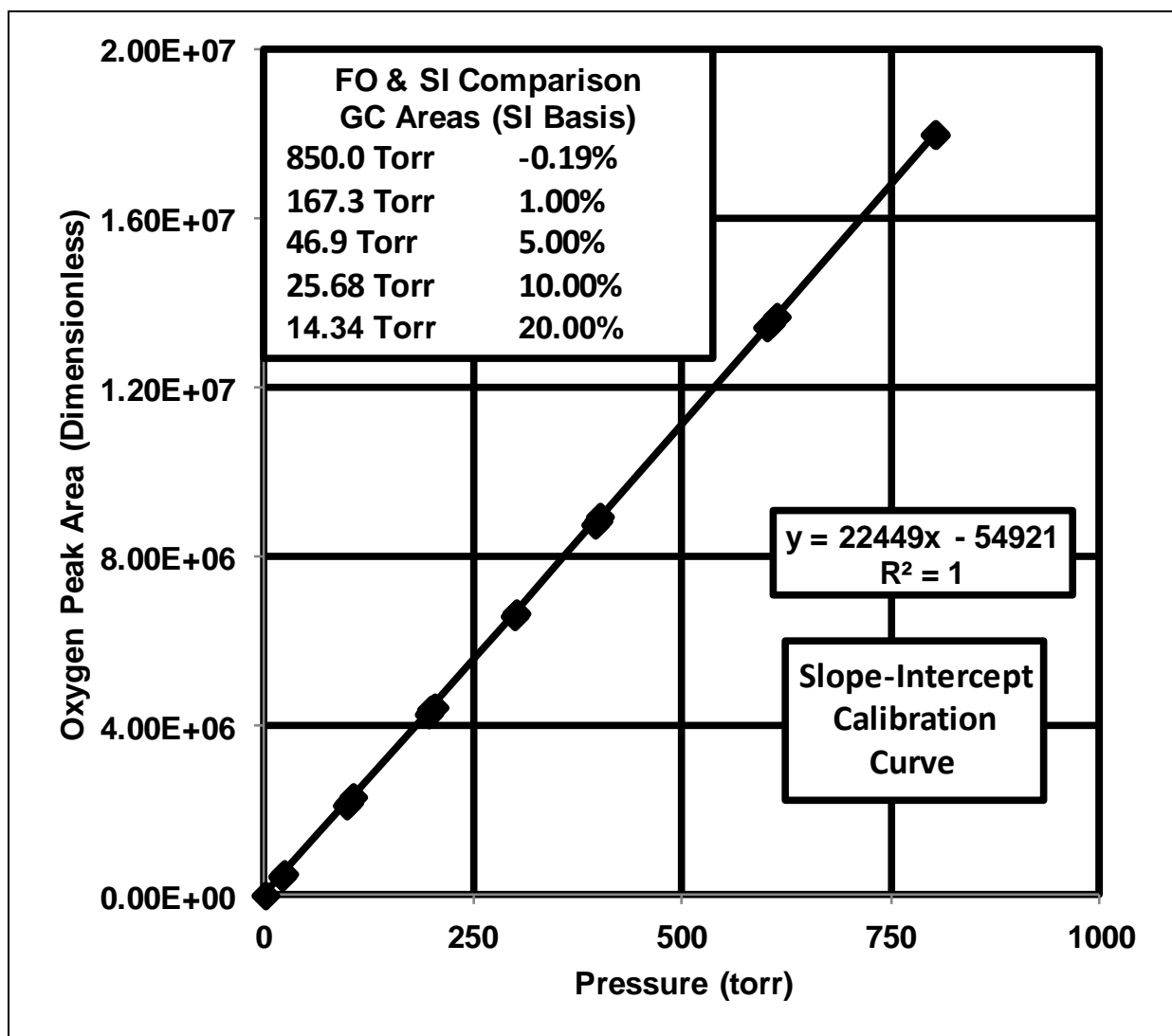


Figure 2. Calibration curve (2013) for pure O₂ gas – slope/intercept method (FO = forced origin, SI = slope-intercept).

The original Agilent 7890A GC slopes for the six thermal battery gases as measured in 2010 are shown in table 1 (row 1). Sometime after the original GC calibration, the GC column and sample inlet tube were both removed during the course of another GC/MS project and then reinstalled. When the column and sample inlet tube were reinstalled, the column sensitivity had decreased by a factor of 1.5200 (2013 O₂ calibration). No gas leaks or other anomalies could be found, and the column was still usable with the reduced sensitivity. Accordingly, the GC was recalibrated using the same column in 2013, again with the curves forced through the origin for direct comparison with the original calibration.

Table 1. Slopes of dimensionless chromatographic peak areas (forced origin method) vs. measured gross gas sample pressures for pure gases and for gases from the certified calibration gas cylinder (including certified calibration cylinder volumetric gas percentages).

GC Calibration Slopes Dimensionless Chromatographic Area vs MKS Pressure (torr)						
Gas	H₂	O₂	N₂	CO	CH₄	CO₂
Pure Gas Slopes (2010)	228411	33960	26009	25178	93933	26684
Initial Pure Gas Slopes (2013)	165741	22342	17524	16564	61798	17555
Effective Slopes for Sample Gas Cylinder (2013)	67180	9056	7103	6714	25049	7116
Final Slopes for Pure Gases Using Sample Gas Cylinder Correction (2013)	160450	21629	16964	16036	59825	16995
Volumetric Percentages of Gases in Cylinder Mixture (Gas Volume Ratios are 0.4187 (Total Sample) /0.5813 (Argon Balance)) Gas Volume Percentages Below are Correct to 2.95% of Each Individual Gas Percentage Shown						
Individual Gas Percentages Present in Sample Gas Cylinder	3.64	2.95	4.77	11.5	4.01	15

Because of limited time during FY 2013, pure gases except for O₂ were not recalibrated comprehensively. An example showing the 2013 calibration curve for pure O₂ gas is shown in figure 1. Pure gas H₂ and N₂ slopes were partially recalibrated to confirm the approximate loss in sensitivity by a factor of 1.52 and found to require additional divisional correction factors of 0.906657 and 0.976455, respectively, in order to obtain the slopes found in the second row of table 1. Then the remaining 3 gas slopes from the 2010 calibration for CO, CH₄, and CO₂ were divided by 1.52 to get slopes that were approximately correct for those remaining 3 gases as shown in table 1 row 2.

The composition of the certified sample gas cylinder was then assumed to be correct and was used as the final 2013 calibration standard for all six sample cylinder gases as shown in table 1 rows 3 and 4. This final calibration reduced the slopes of all six pure gases equally by a factor of 1.03297 by using the fact that the sum of the pressures of the individual gases measured chromatographically should equal the total physical gas sample pressure as measured by the MKS DCM after allowing for the 0.5813 volume fraction of argon that was present in the certified sample gas cylinder. All of the slopes shown in table 1 row 3 can be obtained by multiplying the respective slopes in table 1 row 2 by 0.4187 and then dividing each result by 1.03297 after allowing for rounding errors in the last digit. Examples showing measurements of the certified gas mixture that confirm the 2013 calibration are shown and briefly explained in tables 2 through 5 and their captions. Note that adding the individual volume gas percentages in

the certified gas cylinder shown in table 1 gives a total percentage of 41.87, which is the total volume percentage of gas sample in the cylinder. Note also that the total gas pressures shown in table 2 and each individual gas pressure shown in table 3 all include proportionate amounts of the 0.5813 fraction of the argon carrier gas present in the certified gas cylinder. Finally, note that dividing the individual effective gas slopes for the sample gas cylinder correction (table 1 row 3) by 0.4187 gives the final slopes for the pure gases calibrated in 2013 after allowing for rounding errors in the last digit (table 1 row 4).

The slopes shown in table 1 row 4 were then used to measure the percentages of gases evolved from vendor thermal batteries during 2013. The individual gas pressures measured chromatographically were used to calculate the individual percentages of each gas in a sample, with the sum of the chromatographically determined pressures for all six gases taken as 100% of the gross gas pressure measured for the total sample. For all of the 2013 thermal battery gas evolution tests, the sum of the pressures of the six gases measured chromatographically was within about 6% of the total sample physical gas pressure measured by the DCM as expected which served as an additional confirmation of the slopes shown in the final 2013 calibration of table 1 row 4.

Table 2. Chromatographic curve areas (dimensionless) measured using the 50 μ l sample loop for the certified gas cylinder calibration tests. These measured gas pressures all include the 0.5813 total volume fraction of argon gas in the certified gas cylinder.

Sample Number	Pressure (Torr)	Dimensionless Chromatographic Peak Area					
		H ₂	O ₂	N ₂	CO	CH ₄	CO ₂
1	592.2	3435705	360455	559202	1097829	1352118	1378216
2	768.4	4625492	479871	665832	1498489	1826613	1910960
3	595.6	3571457	370630	514605	1141635	1381793	1442749
4	601.9	3474988	357738	545900	1089317	1420274	1395987
5	604.5	3428201	383556	570908	1097285	1458814	1435975
6	610.2	3650606	377210	588026	1167934	1453381	1523241
7	614.8	3574974	374174	553869	1139167	1567814	1490706
8	608.6	3435013	388972	604628	1105056	1438548	1409861
9	627.6	3495417	397480	633056	1120379	1393729	1449353
10	607.6	3613087	404289	520450	1141444	1429888	1439970
11	631.5	3770049	395020	562309	1204671	1460422	1544820
12	663.6	3959022	401297	623348	1265742	1648416	1647552
13	682.5	4087380	412757	621051	1300479	1583115	1675798
14	651.4	3872279	377733	634870	1261314	1531006	1586720

Table 3. Individual gas pressures (torr) measured chromatographically for the gas samples shown in table 2 and taken from the certified calibration gas cylinder. Each individual gas pressure shown in table 3 includes a proportionate amount of the 0.5813 total volume fraction of argon gas in the certified gas cylinder.

Sample Number	Calculated Pressure of Gas Under Chromatographic Curve (torr)					
	H ₂	O ₂	N ₂	CO	CH ₄	CO ₂
1	51.141	39.803	78.728	163.510	53.979	193.686
2	68.851	52.989	93.740	223.184	72.922	268.554
3	53.162	40.926	72.449	170.035	55.164	202.755
4	51.726	39.503	76.855	162.242	56.700	196.183
5	51.029	42.354	80.376	163.429	58.239	201.803
6	54.340	41.653	82.786	173.952	58.022	214.067
7	53.214	41.318	77.977	169.667	62.590	209.494
8	51.131	42.952	85.123	164.587	57.430	198.133
9	52.030	43.891	89.125	166.869	55.641	203.683
10	53.781	44.643	73.272	170.006	57.084	202.364
11	56.118	43.620	79.165	179.423	58.303	217.099
12	58.931	44.313	87.759	188.519	65.808	231.537
13	60.841	45.578	87.435	193.693	63.201	235.506
14	57.639	41.711	89.381	187.860	61.121	222.988

Table 4. Moles of individual gases contained within the 50 μ l sample loop for the gas samples shown in table 2 and taken from the certified calibration gas cylinder. The experimental temperature was taken at 298 °K for all of the molar calculations shown below. The molar volumes for all of the individual gases are 22.4140 std liter where $V = nRT/P = 1 \text{ mole} \times 62.3638 \text{ (l-Torr/mol-}^\circ\text{K)} \times 273.15 \text{ }^\circ\text{K}/760 \text{ Torr}$.

Sample Number	Moles of Individual Gases					
	H ₂	O ₂	N ₂	CO	CH ₄	CO ₂
1	5.76E-08	4.48E-08	8.87E-08	1.84E-07	6.08E-08	2.18E-07
2	7.76E-08	5.97E-08	1.06E-07	2.51E-07	8.21E-08	3.03E-07
3	5.99E-08	4.61E-08	8.16E-08	1.92E-07	6.21E-08	2.28E-07
4	5.83E-08	4.45E-08	8.66E-08	1.83E-07	6.39E-08	2.21E-07
5	5.75E-08	4.77E-08	9.05E-08	1.84E-07	6.56E-08	2.27E-07
6	6.12E-08	4.69E-08	9.33E-08	1.96E-07	6.54E-08	2.41E-07
7	5.99E-08	4.65E-08	8.78E-08	1.91E-07	7.05E-08	2.36E-07
8	5.76E-08	4.84E-08	9.59E-08	1.85E-07	6.47E-08	2.23E-07
9	5.86E-08	4.94E-08	1.00E-07	1.88E-07	6.27E-08	2.29E-07
10	6.06E-08	5.03E-08	8.25E-08	1.92E-07	6.43E-08	2.28E-07
11	6.32E-08	4.91E-08	8.92E-08	2.02E-07	6.57E-08	2.45E-07
12	6.64E-08	4.99E-08	9.89E-08	2.12E-07	7.41E-08	2.61E-07
13	6.85E-08	5.13E-08	9.85E-08	2.18E-07	7.12E-08	2.65E-07
14	6.49E-08	4.70E-08	1.01E-07	2.12E-07	6.89E-08	2.51E-07

Table 5. Percent errors of individual gases found under chromatographic curves when compared with the certified gas cylinder specifications for the gas samples shown in table 2 and comparisons of DCM total gross gas sample pressures with the sums of the pressures of the individual gases found under the chromatographic curves.

Sample Number	Percent Error						DCM/Chromatographic Area Total Pressure Measurement Difference (%)
	H ₂	O ₂	N ₂	CO	CH ₄	CO ₂	
1	1.28	-2.74	18.97	2.49	-2.97	-6.92	1.92
2	1.51	-3.61	5.46	4.15	-2.41	-3.92	-1.54
3	2.86	-2.29	6.97	4.14	-3.11	-4.80	0.19
4	2.02	-3.86	15.67	1.28	1.51	-6.10	3.11
5	-1.72	0.65	18.13	-0.37	1.82	-5.68	1.20
6	0.04	-5.38	16.30	1.36	-3.04	-4.37	-2.40
7	-0.35	-4.53	11.43	0.57	6.39	-4.80	0.09
8	-1.87	1.71	24.67	-0.02	0.05	-7.73	1.52
9	-2.09	1.92	27.99	-0.60	-4.95	-6.98	2.61
10	2.91	5.40	6.99	2.96	-0.85	-6.04	1.06
11	1.86	-2.31	9.65	3.08	-3.94	-4.38	-0.35
12	0.15	-7.08	13.81	1.40	1.52	-4.52	-2.00
13	1.98	-5.73	11.84	2.76	-3.84	-4.21	-0.55
14	0.35	-10.40	18.75	3.52	-3.41	-5.79	-1.43

O₂ and N₂ show the largest percent errors in table 5 because they elute at similar times and their peaks are difficult to separate. Comparison of the O₂ and N₂ calibration slopes shows that the two slopes are similar. In table 5, the measured N₂ error percentages are usually positive and large, while the measured O₂ error percentages are usually negative or small. Finally, the sums of the pressures of all of the gases as measured by the chromatographic curves closely agrees with the DCM physical measurements of the respective total sample pressures.

Table 5 shows that the percentages of all of the gases except for O₂ and N₂, as determined by this method, are correct to better than $\pm 10\%$. The measured error percentage for H₂ for the 2013 calibration is about $\pm 3\%$ or less as shown in table 5. If the measured volumetric percentage of H₂ in a specified gas mixture were $\pm 10\%$, for example, the true volumetric percentage of the H₂ in that mixture would be somewhere between 9% and 11%. The thermal conductivity values of O₂ and N₂ are similar and those of H₂ are approximately 6 times greater than those of O₂ and N₂ (and of the other 3 gases as well) at pressed pellet thermal battery operating temperatures, so that the relative ratios of N₂, O₂, and the other gases are of less importance so long as the total percentage of H₂ is correct.

Thermal battery gas analysis measurements using the 7890A GC done in 2010 and in 2013 both confirmed previous measurements reported using the HP Series II 5890 GC that were done during and before 2010 (5). The 5890 HP tests had used the same type of column (Carboxen 1010 Supelco PLOT capillary column) and a very similar GC operating method. The MS was

used to qualitatively identify gases from thin-film thermal battery research programs. Quantitative MS analyses for the research thin-film thermal battery program are in progress.

4. Vendor Thermal Battery Gas Evolution

After the pure gas and gas mixture slopes were confirmed and correlated, the final slope values for pure gases (table 1 row 4) were used to determine the partial pressures of the above six gases in pressed pellet vendor thermal battery operating atmosphere gas samples. Initial gas samples were typically taken into an evacuated open 10-cc SS sample bottle immediately after battery ignition. Additional gas samples would then typically be taken every few minutes after ignition for 10 or 15 min. Intermittent gas samples might then be taken a few hours after battery ignition until approximately 24 h after ignition to check for reactions of the gases with the expended thermal battery components.

The summed partial pressures of the six gases (H_2 , O_2 , N_2 , CO , CH_4 , and CO_2) evolved from all of the pressed pellet munitions thermal batteries, as determined from the calibrated GC peak areas, agreed to better than 94 % with the total physical pressures of the respective gas samples when measured by the DCM. This showed that those six gases constituted more than 94 % by volume of the evolved gases from the pressed pellet munitions thermal batteries and served as an additional check of the 7890A GC calibration. For all of the pressed pellet thermal batteries tested, H_2 gas concentrations showed a gradual decrease during battery discharge, while CH_4 showed an increase in concentration.

The amounts of H_2 gas found in the operating pressed pellet vendor thermal battery gas atmospheres were sufficient to increase the global thermal conductivity values of even the most efficient presently used microporous thermal battery thermal insulation packages by factors ranging from 1.5 to 3 during battery operation as has been reported previously (*1, 4*). If less expensive non-microporous thermal insulation is used, gross thermal battery thermal insulation package thermal conductivity values might be increased by as much as a factor of about 6 by H_2 gas evolution. If H_2 can be removed, these increases in thermal insulation package thermal conductivity values during battery operation will not occur and vendor thermal battery thermal and electrical lifetimes can be increased accordingly. Thermal modeling shows that thermal lifetimes can be increased in essentially direct proportion to any reduction in the gross thermal insulation package thermal conductivity values.

Thin-film thermal batteries tested showed either greatly reduced or greatly elevated and unacceptable gas pressures, depending on the thermal battery design, materials, battery construction, and chemical processing methods. Some thin film thermal battery designs evolved only the gases found in the pressed pellet thermal batteries. Other thin-film battery designs evolved additional gases identified by the MS but not yet quantified.

5. Summary and Conclusions

GC/MS methods were confirmed, calibrated, and used during 2013 and the GC/MS is available for other ARL projects as appropriate. Immediate chemical identification of gaseous (and liquid) materials can be achieved directly from the GC/MS local area network control computer (Chemstation) using previously stored National Institute of Standards and Technology (NIST), Occupational Safety and Health Administration (OSHA), Massachusetts Institute of Technology (MIT), Cornell, and other MS libraries. Custom (user) and Agilent locked libraries can also be placed on the Chemstation.

Chromatographic gas analyses of vendor munitions thermal batteries combined with previous thermal insulation thermal conductivity measurements confirmed that the presence of H_2 gas in operating vendor munitions thermal batteries presents a significant heat transfer problem for pressed pellet munitions thermal batteries (1, 4). Thermal modeling clearly shows that just the removal of H_2 gas with no other changes could immediately improve the lifetimes of many pressed pellet munitions thermal battery applications by factors ranging from 1.5 to 3 even when using highly efficient microporous thermal insulators. If less expensive non-microporous thermal insulators are used, some thermal battery munitions application lifetimes might be improved by factors of as much as 6. For many vendor munitions thermal batteries of a given volume, thermal lifetimes can be increased in direct proportion to the global thermal insulation package thermal conductivity by using appropriate gas control and battery construction methods with thermal modeling. More complete gas control methods combined with thermal modeling can have much more significant effects (6).

Vendor participation in gas control/thermal modeling efforts is essential to the optimization of vendor thermal batteries, but many vendor thermal batteries might be improved significantly simply by adding $BaCrO_4$ and heat paper to the thermal insulation package. $BaCrO_4$ was used to remove 94 % or more of H_2 evolved from heat paper (2). The H_2 gas present in the operating LCCM thermal battery did not increase measurably during battery operation, which highly suggests that significant amounts of additional H_2 gas were not formed from the water vapor shown to be present (1, 4). Traditional munitions thermal battery gas removal methods such as materials choices, chemical processing methods, battery construction methods, and internal heat balances can all help to remove H_2 gas. Gas getters can also be used to reduce H_2 levels in operating munitions thermal batteries.

Work is in progress to confirm the Sierra thermal battery finite element thermal models using previously proven ARL Fortran heat transfer optimization programs. More rigorous gas control methods, combined with proper thermal modeling and battery construction methods could ultimately eliminate heat transfer as a major limiting factor in munitions thermal battery lifetimes.

6. Future Work

Additional thin-film thermal batteries will be tested for gas evolution. Both nanofoil and traditional pressed heat pellets will be used as heat sources for thin-film thermal batteries. Quantitative GC and MS analyses of thin-film and traditional pressed pellet thermal batteries will be continued. The Sierra finite element thermal model will be confirmed using previously proven ARL Fortran thermal battery optimization programs. Gas evolution studies will continue and gas control methods will be applied to a working LCCM thermal battery during 2014.

An improved gas handling system for pressed pellet munitions thermal battery testing is shown in figure 3. Additional sample bottles have been added to reduce possible breaches of the GHS during battery testing.

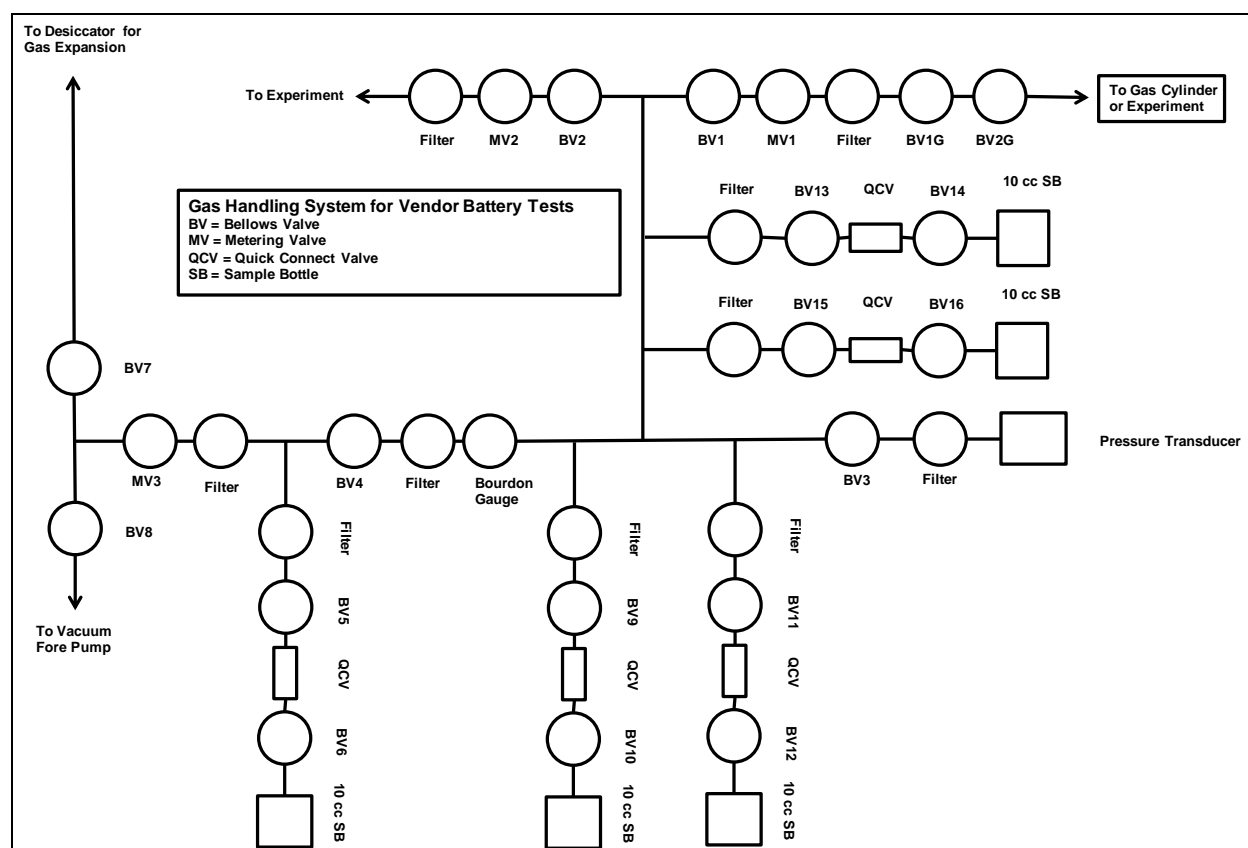


Figure 3. Schematic of enhanced gas handling system for use during 2014.

7. References

1. Krieger, F.; Ding, M. *Thermal Battery Operating Gas Atmosphere Control and Heat Transfer Optimization*; ARL-TR-6156; U.S. Army Research Laboratory, Adelphi MD, September 2012.
2. Krieger, F. et al. Gas Control Experiments and Calculations for Pressed Pellet Thermal Batteries. *Proc. 45th Power Sources Conference*, 551, July 2012.
3. Krieger, F., et al. Gas Evolution from Thermal Battery Materials. *Proc. 44th Power Sources Conference*, 517, July 2010.
4. Krieger, F.; Ding, M. *Heat Transfer in the LCCM Thermal Reserve Battery*; ARL-TR-4843; U.S. Army Research Laboratory, Adelphi MD, September 2009.
5. Krieger, F.; Lennen R. Practical Miniaturization of the LCCM Thermal Battery using Gas Getters. *Proc. 42nd Power Sources Conference*, Philadelphia, PA, 2006, 253.
6. Krieger, F. Miniature Thermal Batteries for Low-Current Applications. *45th Annual NDIA Fuze Conference Presentation*, Long Beach, CA, 2001.
7. McIntyre, R. *Procedure for Determination of Gas Evolved by Thermite Mixtures*; TR-702; Diamond Ordnance Fuze Laboratories, Washington DC, February 1960.

List of Symbols, Abbreviations, and Acronyms

ARDEC	Armament Research, Development, and Engineering Center
ARL	U.S. Army Research Laboratory
BaCrO ₄	barium chromate
CH ₄	methane
CO	carbon monoxide
CO ₂	carbon dioxide
DCM	dual capacitance manometer
GHS	gas handling system
GC	gas chromatograph
H ₂	hydrogen
HP	Hewlett Packard
LCCM	Low Cost Competent Munition
MIT	Massachusetts Institute of Technology
MS	mass spectrometer
N ₂	nitrogen
NIST	National Institute of Standards and Technology
O ₂	oxygen
OSHA	Occupational Safety and Health Administration
PLOT	porous layer open tubular
SS	stainless steel
TPA	Technical Program Annex
UHP	ultra high purity

1 (PDF)	DEFENSE TECHNICAL INFORMATION CTR DTIC OCA	3 (PDFS)	SANDIA NATIONAL LABORATORIES DANIEL WESOLOWSKI EDWARD PIEKOS ANNE GRILLET
1 (PDF)	GOVT PRINTG OFC A MALHOTRA	2 (PDFS)	ADVANCED THERMAL BATTERIES INC DOUG BRISCOE JEFFREY REINIG
1 (PDF)	US ARMY ARDEC ATTN AMSRD AAR MEF S C MCMULLAN	3 (PDFS)	ENERSYS ADVANCED SYSTEMS PAUL SCHISSELBAUER ANDREW SEIDEL TIM HURST
1 (PDF)	US ARMY ARDEC ATTN RDAR EIF C JANOW	3 (PDFS)	EAGLE PICHER TECHNOLOGIES LLC JIM FERRARO CHARLEY LAMB DHARMESH BHAKTA
2 (PDF)	US ARMY ARDEC ATTN RDAR MEF F K AMABILE ATTN RDAR MEF F R DRATLER	3 (PDFS)	THE ENSER CORPORATION ROY JACKSON NICK SHUSTER DAVE NIERMAN
1 (PDF)	CDR US ARMY TACOM ARDEC ATTN AMSRD AAR AEP E D TROAST	1 (PDF)	VACUUM ENERGY, INC. RICHARD KULLBERG
1 (PDF)	US ARMY ARDEC ATTN RDAR MEF E G SALATHE		
2 (PDFS)	US ARMY ARDEC B ARMSTRONG M ALLENDE		
16 (PDFS)	US ARMY RSRCH LAB ATTN RDRL SED C M S DING ATTN RDRL SED C C LUNDGREN ATTN RDRL SED C F KRIEGER ATTN RDRL SED C J SWANK ATTN RDRL SED C D BAKER ATTN RDRL SED C I LEE ATTN RDRL SED C A BOOTH ATTN RDRL SED C D TRAN ATTN RDRL SED C J READ ATTN RDRL SED C J WOLFENSTINE ATTN RDRLSED E E SHAFFER ATTN RDRL SED E J MULLINS ATTN RDRL SES S A LADAS ATTN RDRL SES X J HOPKINS ATTN IMAL HRA MAIL & RECORDS MGMT ATTN RDRL CIO LL TECHL LIB		

INTENTIONALLY LEFT BLANK.